Z-RNA and the flipside of the SARS Nsp13 helicase

Alan Herbert[1,2*] and Maria Poptsova[2]

[1]InsideOutBio, 42 8th Street, Charlestown, MA

[2] Laboratory of Bioinformatics, Faculty of Computer Science, National Research University Higher School of Economics, 11 Pokrovsky Bulvar, Moscow, Russia 101000

*Corresponding author

alan.herbert@insideoutbio.com

Keywords: coronavirus;SARS;MERS;Z-RNA;ZBP1;Necoptosis

Abstract

We present evidence that the severe acute respiratory syndrome coronavirus (SARS) non-structural protein 13 (Nsp13) modulates the Z-RNA dependent regulated cell death pathways [1]. We show that Z-prone sequences (called flipons [2]) exist in coronavirus and provide a signature (Z-sig) that enables identification of the animal viruses from which the human pathogens arose. We also identify a potential RIP Homology Interaction Motif (RHIM) in the helicase Nsp13 that resembles those present in proteins that initiate Z-RNA-dependent cell death through interactions with the Z-RNA sensor protein ZBP1. These two observations allow us to suggest a model in which Nsp13 down regulates Z-RNA activated innate immunity by two distinct mechanisms. The first involves a novel ATP-independent Z-flipon helicase (flipase) activity in Nsp13 that differs from that of canonical A-RNA helicases. This flipase prevents formation of Z-RNAs that would otherwise activate cell death pathways. The second mechanism likely inhibits the interactions between ZBP1 and the Receptor Interacting Proteins Kinases RIPK1 and RIPK3 by targeting their RHIM domains. Together the described Nsp13 RHIM and flipase activities have the potential to alter the host response to coronaviruses and impact the design of drugs targeting the Nsp13 protein. The Z-sig and RHIM domains may provide a way of identifying previously uncharacterized viruses that are potentially pathogenic for humans.

Introduction

Human Coronaviruses. Seven human coronaviruses (hCoV) of the order *Nidovirales* are known to infect humans [3; 4; 5]. These include two alpha-coronaviruses (hCoV-229E (229E)and hCoV-NL63 (NL63)) and five beta-coronaviruses (SARSCoV (SARS1), SARS-CoV-2 (SARS2), MERS-CoV (MERS), hCoV-HKU1 (HKU1), and hCoV-OC43 (OC43)) (Figure 1A). The HKU1, 229E, NL63 and OC43 viruses produce mild symptoms while SARS1, SARS2 and MERS cause severe acute respiratory syndrome (SARS). Much interest has focused on factors that contribute to the morbidity and mortality associated with pathogenic CoV. These include those proteins produced by the virus to counter host responses to the viral double-stranded RNA produced during replication. For example, viral Non-Structural Proteins (NSP) Nsp4a and 4b of MERS suppress induction by double-stranded RNA (dsRNA) of interferon lambda 1 gene expression [6]. A number of other CoV countermeasures interfere with host interferon responses (summarized in [7]). Host factors also increase the severity of disease, including genetic variants that reduce IFN responses and auto-antibodies that inhibit IFN activity [8; 9; 10].

CoV are long (~30Kb) positive strand, single-stranded RNA (ssRNA) viruses that replicate themselves within double membrane vesicles through a dsRNA intermediate [4; 11]. The RNA-dependent RNA polymerase (RdRp) involved in genome replication also creates sub-genomic negative strand templates to direct production of structural proteins necessary for virion assembly. The sub-genomic RNAs share the same leader sequence, which is encoded in the 5′ end of the viral genome and joined to a downstream open reading frame (ORF). All the genomic sequence in between that encode the NSPs are excluded. The production of sub-genomic templates depends on transcription regulatory sequences (TRS), such as the AACGAAC sequences present in beta-coronaviruses (Figure 1A). Switching of the RdRp from a downstream TRS to that associated with the leader sequence involves a long-distance RNA interaction [12]. Since replication of the 30Kb CoV genome and the generation of sub-genomic RNAs have the potential to generate sufficient topological stress able to power the flip of right-handed A-RNA

25 to left-handed Z-RNA, we were interested in the role played by the Z-RNA sensor protein ZBP1
26 (historically called Z-DNA Binding Protein 1) in CoVs infection. After describing Z-DNA and Z-RNA (ZNA)
27 more fully, we propose evidence-based mechanisms through which CoV suppresses Z-RNA dependent
28 inflammatory responses.

29 **Z-RNA and Flipons.** The left-handed Z-DNA and Z-RNA (ZNA) conformations form from their right-
30 handed counterparts of B-DNA and A-RNA by flipping the bases over to produce the characteristic zig-
31 zag backbone of these reverse-twisted, double-stranded nucleic acid conformers [13]. The energy to
32 power the flip can arise from the negative supercoiling produced in the wake of processive enzymes
33 such as helicases and polymerases. In other situations, the topological stress necessary to initiate the
34 ZNA flip is produced by base pairing of entangled nucleic acids, as can occur in stress granules and with
35 defective viral genomes [14] .Sequences that form ZNA under physiological conditions are called flipons.
36 They are often composed of alternating pyrimidine and purine residues, such as $(CG)_n$, $(CA)_n$ and $(UG)_n$.
37 The propensity of flipons to adopt the ZNA conformation can be scored using the ZHUNT3 (ZH3)
38 program [15]. Much of the energy cost in ZNA formation is in the creation of junctions between right-
39 handed and left-handed helices. For Z-RNA, the flip occurs more easily when dsRNA contain basepair
40 mismatches, non-canonical basepairs or unpaired residues at both ends of the Z-forming segment [16].

41 **Z-RNA and innate immunity.** Z-DNA and Z-RNA are recognized in a conformation specific manner by
42 proteins containing the Zα domain, which was first discovered in the dsRNA editing enzyme ADAR1 [17].
43 The Zα domain is also found in many other proteins, including ZBP1 and virally encoded proteins like
44 vaccinia virus E3 [18] and African swine fever virus [19]. Interaction between Zα proteins regulates cell
45 death pathways [20; 21] (Figure 1B). The pathways are triggered by binding off ZNAs to ZBP1, which
46 then activates RIPK1 and RIPK3 through the RIP Homology Interaction Motifs (RHIMs) shared by all three
47 proteins. RIPK3 once activated by ZBP1 then phosphorylates Mixed Lineage Kinase Domain Like
48 pseudokinase (MLKL) to promote pore formation in cell membranes, producing an inflammatory form of

49 cell death called necroptosis. ZBP1 activation of RIPK1 on the other hand induces Caspase-8-dependent
50 apoptosis, via the adaptor protein FADD and inhibits necroptosis [20; 21].

51 The RHIM is a ~40 aa motif, first identified in RIPK1 [22], that contains an (I/V)Q(I/L/V)G sequence at its
52 core [23] (Figure 1C). Structural studies have revealed the nature of how RHIMs interact with each
53 other. The two hydrophobic residues (colored yellow in Figure 1C) of the first RHIM interdigitate with
54 those on a second RHIM to anchor the interaction. The complex is further stabilized by glutamine and
55 other residues (colored in blue) that seal the core and promote the formation of higher order
56 dimensional structures that resemble amyloid fibrils. While RIPK1 and RIPK3 can form homomeric fibrils,
57 they also can stack on top of one another to scaffold assembly of cellular machines that initiate
58 downstream pathways [24; 25; 26].

59 V**iruses and ZBP1 dependent necroptosis.** The ZBP1-initiated cell death pathways plays an important
60 role during infection by the negative RNA stranded influenza virus [27], as well as upon infection with
61 the herpesviruses murine cytomegalovirus (mCMV), human herpes simplex viruses (HHSV) and the
62 vaccinia poxvirus [28]. These viruses have developed a number of strategies to regulate ZBP1-dependent
63 cell death. These include the encoding of ZBP1 homologs, such as the E3 protein, that compete with
64 ZBP1 for ZNAs [28] and proteins with RHIMs that target the ZBP1 and RIPK1/RIPK3 interactions. So far,
65 only RHIMs produced by DNA viruses like the human Herpesviridae (HHV) and mouse cytomegalovirus
66 (CMV) are known to play an important role in virulence [29]. Notably, no RNA virus has yet been shown
67 to encode a RHIM-containing protein.

68 **Results**

69 **A corona virus-specific Z-flipon signature.** We were interested in whether the SARS family
70 coronaviruses might also induce Z-RNA dependent ZBP1 activation and cell death. We used a two-
71 pronged approach. First, we searched for Z-prone sequences in coronavirus using the program ZH3 [30].

72 We were interested in those sequences that characterize highly pathogenic CoV. Second, we searched
73 for RHIMs in CoV proteins.

74 **Coronavirus Z-prone sequences.** We found that all examined coronaviruses contained sequences that
75 were Z-prone, and that the Z-signature (Z-Sig) for each strain of virus is unique (Figure 1). Using the
76 signature, it is easy to identify the host animal from which the pathogenic human viruses arose. For
77 example, we show that the signatures for Llama coronavirus (CoV) and MERS are identical, as are those
78 for civet CoV and SARS1, as well as those for bat-RaTG13 and SARS2 (Figure 1 Panels A and B). The Z-sigs
79 that characterize each strain are present throughout the genome. Those present in the NSP coding
80 regions of the genome help identify SARS1 and MERS strains, with strong Z-RNA prone regions are also
81 present in the sub-genomic RNAs of both MERS and SARS2.

82 The ZH3 scoring is based on the energetics of Z-DNA flipping, where a score greater than 600 is sufficient
83 to change flipon conformation under physiological conditions. While not experimentally calibrated for
84 the formation of Z-RNA, the scores observed for the CoVs are far in excess of this value and it is likely
85 that the sequences in these viruses constitute flipons. With this caveat in mind, we analyzed Z-prone
86 sequences in CoV strains after sequence alignment to the SRAS2 genome, retaining gaps in the output
87 and examine sequences that were present in two or more strains. We also aligned individual CoV gene
88 sequences separately to correct mistakes in the whole genome analysis that arise because of the
89 different sizes in the genome (Figure 3). As expected from the Z-Sigs, the patterns of Z-RNA prone
90 sequences were similar between SARS1 and civet, between SARS2 and Bat-RaTG13 and between MERS
91 and llama-Qatar15.

92 We analyzed ten of the Z-sig regions identified further. Five Z-sigs were present in genetic regions highly
93 conserved between strains. These encode the Nsp12, Nsp13, Nsp14, S and M proteins. The Nsp13
94 protein (highlighted in the red box of Figure 3A) is a helicase essential for genome replication and

95 transcription. Its genomic sequences contained the highest Z-Score for SARS1. The score for the
96 equivalent region in SARS2 was lower due to three synonymous mutation in adjacent codons that
97 preserve a hairpin sRNA structure and the encoded peptide PARAR (amino acid (AA) residues 335-339 of
98 SARS2 Nsp13) (Figure 3B). This arginine rich peptide sequence has the potential to bind nucleic acids
99 (figure 2A and B) [31]. The equivalent region of MERS Nsp13 contained a sequence that was less Z-prone
100 and coded for the peptide PAKAR that contains the conservative substitution of lysine (underlined) for
101 arginine. Another highly conserved Z-prone sequence was found in the Nsp12 (RdRp) gene, within the
102 region encoding the NiRAN domain. This domain catalyzes the NMPylation of the strongly conserved N
103 terminus of Nsp9, a modification essential for CoV genomic replication [32]. Although there were
104 nucleotide differences between SARS1 and SARS2, they did not alter the AA sequence. The alternating
105 pyrimidine/purine stem formed by folding the RNA is 11 basepair (bp) in SARS1 rather than 9 bp in
106 SARS2. Another Z-prone sequence was found in Nsp14 and is conserved in strains with different hosts.
107 The Z-prone sequence maps just before the flexible hinge region of the guanine-N7-methyltransferase
108 domain that synthesizes the 5´-terminal cap structure essential for viral mRNA translation [33]. A Z-
109 prone sequence was also present in the region that codes for the S2 ectodomain of the spike protein.
110 The peptide produced includes cysteine 851, which forms a disulfide bond with residue 840 (residues
111 822 and 833 in SARS), creating a loop that regulates membrane fusion of the virion with the cytoplasmic
112 membrane of the host [34]. Another Z-prone sequence is present in the highly conserved M gene. The
113 segment encodes the membrane protein's carboxy-terminus AAs that lie just inside the viral envelope.
114 The M-protein interacts with all other structural CoV proteins and is the most abundant protein
115 produced. The protein shapes the virion structure and stabilizes the nucleoprotein (N) protein-RNA
116 complex [35].

117 With regard to other changes in Z-prone sequences, 5 were highly variable between strains. Nsp1 and
118 Nsp2 sequences were quite diverse with some Z-prone sequences encoding an alanine/arginine dimer

119 (AR), suggesting that there regions interact with RNA [31]. Within Nsp1, the Z-prone sequences were
120 present at the amino terminus, a region identified as key to inhibiting the translation of cellular proteins
121 through interactions with the ribosome and critical to a productive viral infection [36]. Nsp1 is thus
122 subject to selective pressures that varies by host. Nsp2 contains two Z-prone sites. The protein is known
123 for its poor sequence conservation with only the zinc finger domain preserved [37]. Another Z-sig is
124 present in Nsp3, which is quite a long gene that also varies in composition between CoV strains [38] The
125 Z-prone sequence in SARS1 Nsp3 encodes part of the macro-1 domain that is involved in de-mono- and
126 de-poly-ADP-ribosylation. The SARS2 sequence is VCVDTVRTN while the SARS1 sequence VCVQTVRTQ,
127 differing by the two residues underlined. These amino acid changes do not directly involve the active
128 site. At the nucleotide level, SARS1 RNA folds on itself to form a 7 bp Z-RNA stem whereas SARS2 RNA
129 does not. Z-prone sequences within the N-protein gene are present in MERS strains. This gene codes for
130 the nucleoprotein involved in packaging the viral RNA into the virion. The Z-sig encode part of the
131 unstructured C-terminus of the protein, beyond the domain critical for RNA packaging that has been
132 characterized in crystallographic studies [39]. The Z-sig encoded residues RTRTR (395-399) do have an
133 alternating motif similar to the KAKAK motif that is specific for Z-RNA [40], potentially allowing
134 interacting with Z-prone sequences in that genome, possibly phasing the sites in the genome to which
135 the N-protein binds.

136 **A putative RHIM associated with coronaviruses severely pathogenic in humans.** In assessing the
137 potential for Z-RNA dependent responses, we searched for viral proteins containing a RHIM that could
138 modulate cell death pathways through interactions such as those illustrated in Figure 1. A multiple
139 sequence alignment showed that Nsp13 in MERS, SARS1 and SARS2 have similar features to known
140 functional RHIMs that are absent in the 229E, OC43, NL63 and HKU1 CoVs (Figure 4A). The residues are
141 colored as in Figure 1C with the core motif in yellow and the other residues that seal the fold in blue.
142 The gray box highlights the labels for previously identified RHIMs. The potential RHIM identified in the

143 nonsense mediated decay associated (NMD) kinase SMG1 [41] is currently undocumented. Other
144 potential RHIMs in Nsp14 (VGTNLPLQLGF), in SMG1 (KAVEHNIQIGK) and UPF1 (RPMFFYVQLGQ) did not
145 align well with known RHIM sequences, but warrant further investigation to test their functionality.

146 **The structure of Nsp13 helicase**. Both strategies of looking for Z-prone sequences and RHIMs focused
147 our attention on the Nsp13 helicase and its potential novel role as a Z-flipon helicase (flipase). Nsp13
148 unwinds both DNA and RNA in the 5'->3' direction. It is a member of the helicase superfamily 1B (SF1B)
149 [42]. Along with Nsp12 and other CoV NSP proteins, Nsp13 forms the viral replication-transcription
150 complex. High resolution crystallographic and electron-microscopy structures of Nsp13 have recently
151 been published and show that a second Nsp13 cooperates with the first to enhance translocation of
152 Nsp13 along the CoV genomic RNA [43; 44; 45]. The Nsp13 helicase has two canonical RecA domains
153 between which ATP is bound and through which single-stranded RNA egresses from the complex. Nsp13
154 also has three N-terminal domains that are unique to nidovirus helicases, with a stalk domain
155 connecting a zinc-binding (ZincBD) domain to the 1B domain (Figure 5).

156 The Nsp13 RHIM is present in the 1B domain, which bridges the RecA1 and RecA2 domains. Rather
157 surprisingly, the peptide PARA encoded by the Z-prone sequence that is in the RecA1 domain interacts
158 with the RHIM when the Nsp13 is in the ATP-free closed conformation (Figure 5A). In the active
159 conformation, the RHIM and PARA segments separate to open a channel through which the ssRNA
160 passes (Figure 5B). Further separation of the 1B domain from the RecA2 domain renders Nsp13 unable
161 to translocate on RNA [45]. The cavity created by this separation appears flexible enough to
162 accommodate a dsRNA structure (Figure 5C).

163 The Nsp13 cavity shown in Figure 5C is lined by the residues known to bind ssRNA (shown by white
164 space fill carbons in figure 6A and 6B), both to the phosphate backbone and also in a base-specific
165 manner. Into the newly formed cavity projects the PARA peptide, with R337 and R339 forming a hook

166 (Figure 6A). Also, tyrosine Y205, along with W178, faces the interior of the cavity (Figure 6B). Potentially
167 Y205 and W178 could engage with each other in an edge to face configuration similar to that of Y177
168 and W195 in the Zα domain to form a platen for the conformation-specific recognition of Z-RNA. These
169 findings support a new role for Nsp13 as a flipase that is described further in the discussion below.

170 **Discussion**

171 **CoV Z-RNA prone sequences**. Our analysis reveals a number of Z-RNA prone sequences (Z-sigs) in
172 human CoV that can be used as fingerprints to identify closely related stains to trace their zoonotic
173 origins. The approach is facile without the need for deep sequence analysis or alignment to confirm the
174 relationship and is quite robust to errors in such procedures.

175 The plots in figure 2 show that potential flipons can occur in many locations within the viral genome.
176 The presence often is associated with alanine/arginine dimers that are encoded by the nucleotide
177 sequence GC(G/A)CG(C/T) and likely reflect in part the essential role of these residues in highly
178 conserved interactions of the virus with RNA [31]. Besides serving as codons, Z-sigs could potentially act
179 as flipons. For example, the flip to Z-RNA could relieve the topological stress generated when both the
180 positive and negative strands of the genome are transcribed by viral polymerases, or during template
181 switching, when the genome loops back to align the leader sequence with more distant regions to
182 produce sub-genomic negative strand RNAs. Alternatively, Z-RNA formation in Z-prone sequences may
183 allow the virus to trap proteins involved in host defense and inhibit their activation of cell-death
184 pathways. Likewise, defective viral genomes, where the Z-RNA flip is powered by base-pairing of
185 entangled RNAs, may act as decoys to derail host responses. Z-prone sequences also can occur in more
186 variable regions of the genome, enabling the evolutionary adaptation of the virus to its host, either
187 through amino acid changes that improve protein function or through the flipon mediated retargeting of

188 the host ribonucleoprotein machinery involved in translation in much the same way as the Z-Box of Alu
189 repeat elements regulate ribosomal assembly [13].

190 **The CoV host range and RHIMs**. Of note is that some hosts lack functional Z-RNA dependent
191 inflammatory cell death pathways, so there is less constraint on the available sequence space they can
192 exploit [46]. However, the Z-prone sequences that evolve in these viruses may impair their ability to
193 infect a new species that have intact ZBP1-dependent cell death pathways. Human represents one such
194 challenging host for zoonotic viruses to colonize. The acquisition of a RHIM domain to prevent Z-RNA
195 dependent outcomes may represent a key adaptive strategy that allows SARS1, SARS2 and MERS strains
196 to productively infect humans. The alternative of reducing the number of viral Z-prone sequences
197 requires retooling of the existing protein machinery and many more changes. In the example of SARS2,
198 the Z-forming potential of the SARS1 Nsp3 Z-sig is reduced by non-synonymous mutations, leaving the
199 encoded peptide the same (Figure 3B). It is unknown whether this decrease in the potential to form Z-
200 RNA increased the potential for SARS2 to become pandemic, but viruses like Epstein-Barr virus show
201 selection against Z-DNA forming sequences relative to other HHVs [47].

202 **Novel Nsp13 flipon helicase activity.** Our structural analysis of the potential Nsp13 RHIM raised the
203 possibility that protein has a non-canonical helicase activity that exploits the strand separation occurring
204 during the transition of A-RNA to Z-RNA (Figure 6C). In this case, the unwinding of dsRNA by the flipase
205 can be powered by the free energy stored in Z-RNA rather than depending like a classical A-RNA helicase
206 does on the energy released by ATP hydrolysis (Figure 6C). The activity of the flipase can be further
207 enhanced by base-specific binding to the alternating pyrimidine/purine ssRNA motifs present in Z-prone
208 sequences, like those present in the CAUGU substrate used by Chen et al in their Nsp13 structural
209 studies. [45]. By sequestering such sequences, Nsp13 would impede the formation of the Z-RNA,
210 inhibiting activation of ZBP1 initiated pathways.

211 It also appears from the structural analysis shown in Figure 5 that engagement of Nsp13 by Z-prone
212 sequences exposes the proposed Nsp13 RHIM. The motif is on the opposite face of the 1B domain to the
213 one that binds RNA (Figure 3C). Once sprung loose, the RHIM is free to contact and modulate the
214 activity of ZBP1, RIPK1 and RIPK3 (Figure 1B), much as the RHIMs from HHV-ICP6, mCMV-M45 and
215 varicella virus HHV3-ORF20 RHIMs do. All of these known viral RHIMS promote formation of
216 heteromeric amyloids [48]. The higher order structures of each viral fibril differs, likely reflecting the
217 impact of residues outside the central core (Figure 1C and 4A). While M45 preferentially interacts with
218 RIPK3 and ZBP1 over RIPK1, ORF20 primarily sequesters ZBP1 [49; 50]. These differences alter the
219 functional outcomes. M45 inhibits tumor necrosis factor induced necroptosis and other cell death
220 pathways, while ORF20 diminishes only ZBP1 dependent apoptosis.

221 It is also possible that the RHIM domain of Nsp13 targets other cellular proteins. The RHIM bearing TRIF
222 protein (toll like receptor adaptor molecule 1 encoded by TICAM1) is directly bound by the dsRNA
223 sensor TLR3 but is indirectly recruited to lipopolysaccharide binding TLR4 via the bridging adaptor TRAM
224 [51]. Mice lacking TRIF are highly susceptible to SARS1 infection and show reduced lung function,
225 increased lung pathology, higher viral titers and increased mortality. These outcomes support the
226 possibility that Nsp13 interacts directly with TRIF and recapitulate many features of human disease [52].
227 Another potential RHIM interaction is with SMG1, a host protein that regulates the onset of NMD by
228 phosphorylating for Upf1 protein. CoV are highly susceptible to NMD due to their dependence on and
229 the nature of the sub-genomic RNAs [53]. The vulnerability arises because only the first ORF of sub-
230 genomic transcripts is translated. The rest of the message is seen by the host as a long 3´UTR of the kind
231 susceptible to NMD [54]. Engaging the potential SMG1 RHIM could be one way the virus inhibits NMD
232 and ensures virion components are synthesized in the quantities required.

233 In summary, we propose that Nsp13 is able to prevent ZBP1 activation of cell death pathways in two
234 different ways. First, the helicase prevents the Z-RNA formation required to engage ZBP1 and second,

235 the RHIM domain inhibits activation of cell death pathways by ZBP1 (Figures 1B and 4A). Potentially the
236 Nsp13 RHIM also regulate activation of inflammatory responses by TRIF and prevent initiation of NMD
237 by SMG1.

238 **Disease Implications .**At this stage, we only know of the possibilities and hope that the above
239 hypotheses will provide a framework for further investigation of Nsp13 effects on Z-RNA dependent cell
240 death in properly qualified BSL3 laboratories. If it is found that pathogenic CoVs do indeed produce Z-
241 RNA (as the ZH3 algorithm predicts) and that the RHIM in Nsp13 regulates ZBP1, RIPK3, RIPK1, TRIF or
242 SMG1 signaling, then we suggest that effects will depend on the stage of viral infection. At early stages,
243 suppressing Z-RNA formation and cell death/NMD would enable increased viral replication while
244 diminishing severity of the initial infection. Here the recognition of Z-RNA prone sequences by Nsp13
245 flipase then blocks the viral polymerase until the two RNA strands are fully separated by the classical
246 Nsp13 helicase activity. At later stages of infection, the dsRNA tangles formed as defective viral genomes
247 accumulate may create Nsp13 clusters, leading to the formation of amyloid filaments, then
248 inflammatory cell death as recently reported for *in vitro* and *in vivo* models of SARS2 infection[55].

249 **Coronavirus and Human Pathology.** From our analysis, it seems that the RHIM domain is a requirement
250 for CoV for the successful jump the virus made from its natural host to humans, although not a sufficient
251 one as other mutations that enable engagement of human cell surface receptors are required. The
252 combination in Nsp13 of the RHIM domain with a Z-flipase so far appears unique among human viruses
253 and may account for the extreme virulence of a subset of CoV. The presence of RHIMs in other viruses
254 that are currently poorly characterized may identify them as potential pathogens before they become
255 pandemic in humans, allowing implementation of pre-emptive measures to counter human infections.

256 The susceptibility of humans to SARS and other novel viruses may also depend on each individual's
257 genome as there is a high frequency of gene variants that impact the necroptotic machinery [46]. The

loss of function alleles reported may leave some individuals more vulnerable to CoV infection and enable persistent viral infections that lead to chronic disease outcomes. Genetic data from cases of long covid would allow identification of any suck risk variants.

While Nsp13 inhibitors that target the ATP-binding site are likely to be effective early in CoV infection by inhibiting the classical helicase function of the enzyme, only those compounds that lock the enzyme in a conformational state unable to engage Z-RNA are likely to be effective against the Z-flipase activity.

Methods

The Z-forming potential of the Coronavirus sequences were assessed using ZHUNT3 using the following command line "zhunt3nt 12 6 24" [30]. The structures PDB files 7NIO [43], 6XEZ [44] and 7RDX [45] were visualized using the open access NGLViewer [56]. Amino acid alignments and the Phylogram were prepared using MUSCLE [57] using the following NCBI sequences for MERS (NC_019843.3), SARS1 (NC_004718.3), SARS2 (NC_045512.2), Hum_CoV-229E (KU291448.1), CoV-OC43 (MW587042.1), CoV_NL63 (MG428706.1), CoV-HKU1 (NC_006577), Bat RaTG13 (MN996532), Civet_007 (AY572034.1) and Llama (MN507638), BAT_HKU4 (NC_009019.1), BAT_HKU5 (NC_009020.1), Murine_CoV_MHV/BHKR (KF268339), RAT_Parker (NC_012936.1) and Pangolin (OM009282.1); Tupaiid herpesvirus 1 tCMV (NC_002794.1). The RHIM in the SMG1 was identified using the MEME Suite [58], using the 10 residues incorporating the colored residues shown in Figure 4 as a seed. Sequence alignments were performed using the MUSCLE [57] CLUSTAL OMEGA algorithm for protein sequences and the CLADOGRAM shown in Figure 4B (accessed on March 24th, 2022 at https://www.ebi.ac.uk/Tools/msa/clustalo/ and MAFFT V7 for Coronavirus sequence alignment, using the option to preserve gaps with the others left as the default and accessed online on March 24th, 2022at https://mafft.cbrc.jp/alignment/server/ [59] and motifs produced using the free version of SNAPGene. Structure images were rendered using the NGLViewer [56] and RNAfold was used to render the RNA images shown in Figure 3B [60].

Author Contributions. AH is an international supervisor for the HSE Bioinformatics Laboratory run by MP. AH conceptualized and wrote the paper with suggestions and edits from MP and AH prepared the figures.

Acknowledgements. We thank Sid Balachandran for suggesting the possibility of RHIM domains in SARS2 and for helpful edits to the manuscript. We thank Alexander Shein who works with M.P. and identified the presence of a strong Z-forming sequence in SARS1

Conflict of Interest. *Author AH is the founder of InsideOutBio, a company that works in the field of immuno-oncology. All the authors declare that the research was conducted in the absence of any commercial or financial relationships that could be construed as a potential conflict of interest.*

A.

	AAACGAAC	SIZE (KB)	NCBI
SARS2	+	29903	NC_045512.2
MERS	+	30033	NC_019843.3
SARS1	+	29751	NC_004718.3
Human-229E	–	27022	KU291448.1
-OC43	–	30727	MW587042.1
-NL63	–	27637	MG428706.1
-HKU1	–	29926	NC_006577
Civet	+	29728	AY572034.1
Ilama	+	30033	MN507638
Bat -RaTG13	+	29855	MN996532
-HKU4	+	30286	NC_009019.1
-HKU5	+	30482	NC_009020.1
Mouse	–	31283	KF268339
Rat	–	31286	NC_012936.1

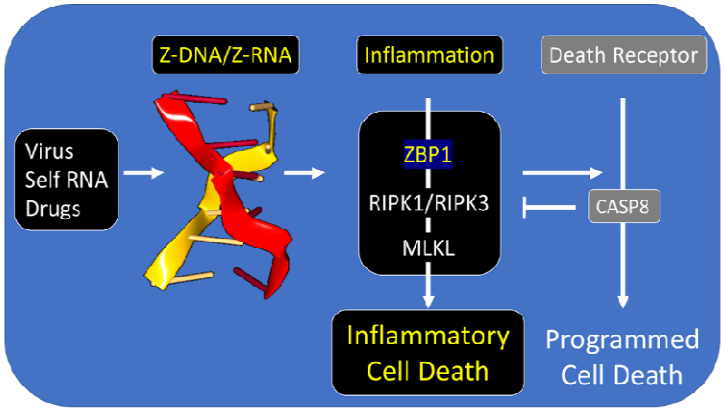

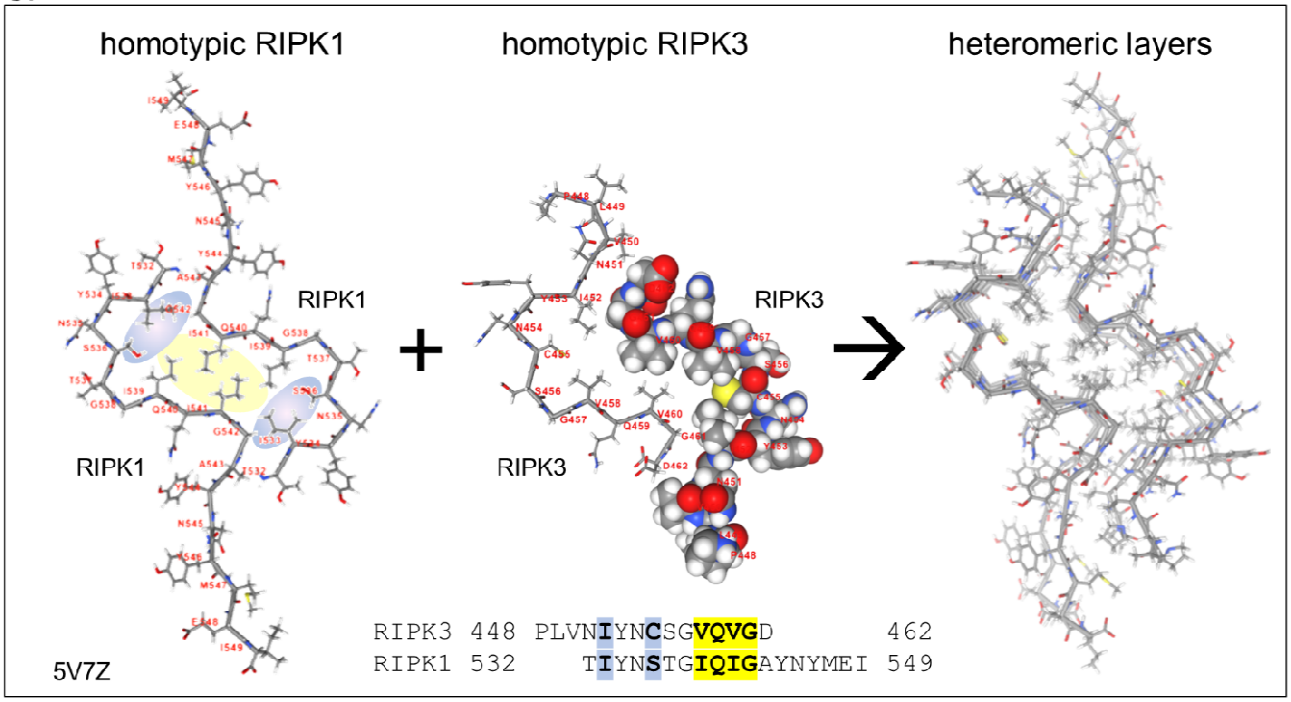

Figure 1. Coronaviruses and human host susceptibility **A.** Coronaviruses (CoV) with the AACGAAC transcription regulatory sequence (TRS) and red labels are associated with severe disease in humans. This TRS is present in CoV from other species but not in all human CoV, especially those that cause mild disease **B.** Host responses to double-stranded Z-RNA viruses can produce inflammatory cell death through the activation of Receptor Interacting Protein Kinases (RIPK) by Z-DNA binding Protein q (ZBP1). The interaction between RIPK and ZBP1 is through their RIP Homotypic Interaction Motifs (RHIM). **C.** Dimers formed from each RHIM protein stack on each other to form a fiber that provides a scaffold for the host response machinery to assemble. The interaction of RIPK1 and RIPK3 is shown with the sequences contributing to the hydrophobic core highlighted in yellow. Blue highlights other residues that stabilize the score. The central figure shows a space-fill representation of one RIPK3 chain present in the dimer.

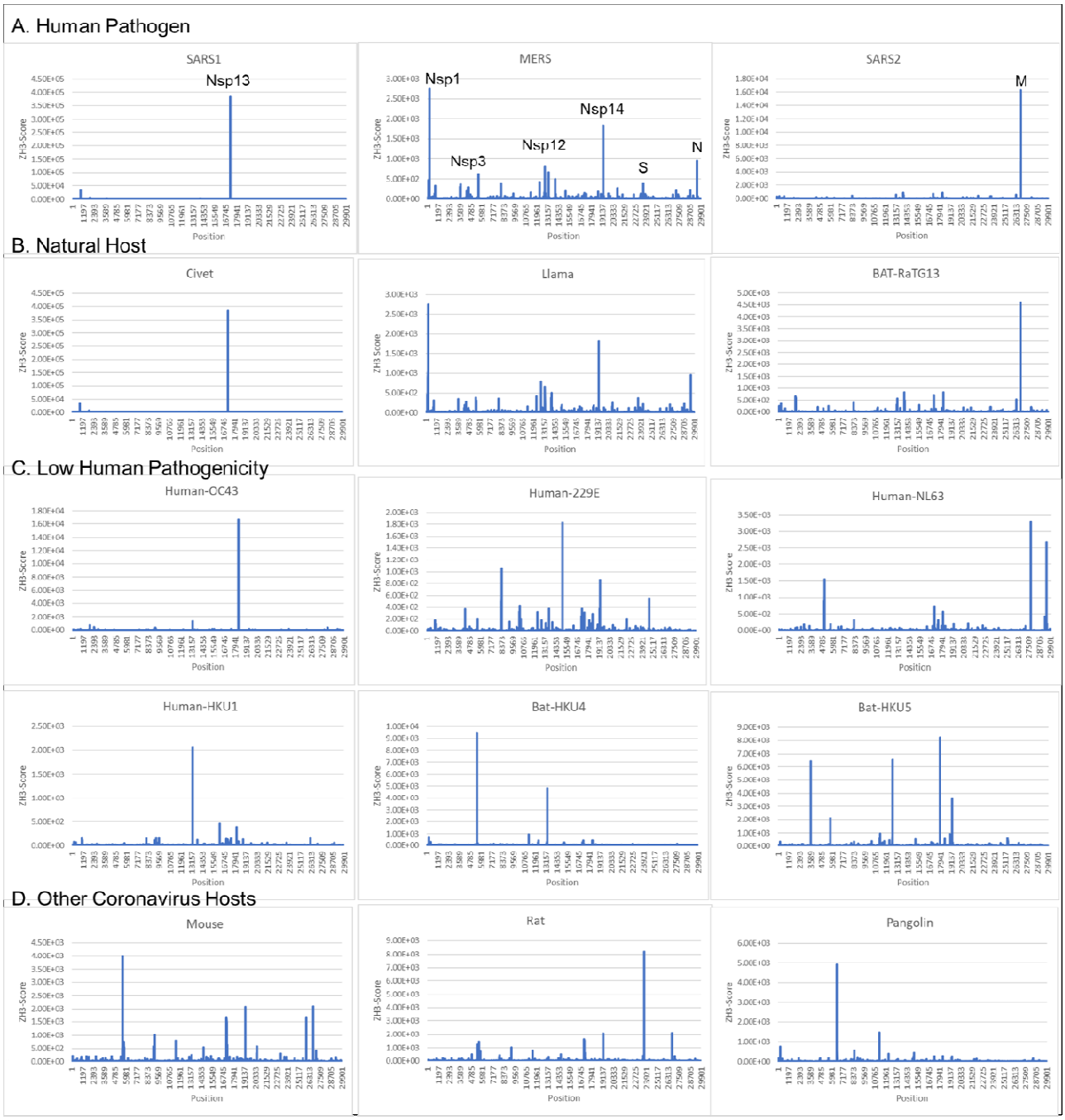

Figure 2. Coronavirus signatures (Z-sigs) based on Z-flipons **A.** Z-sigs for each human pathogenic virus are unique. **B.** Z-sigs match those for the presumed natural hosts for each virus. **C.** The Z-Sigs differ from those for other known coronaviruses **D.** The Z-sigs also vary with the host animal infected. The Z-sig was derived using the ZHUNT3 (ZH3) program [15] that scores the propensity of sequences to flip to the left-handed helical Z-conformation. Sequences with a score greater than 600 are likely to adopt the Z-conformation under physiological conditions. Sequences were aligned using MAFFT prior to analysis [59].

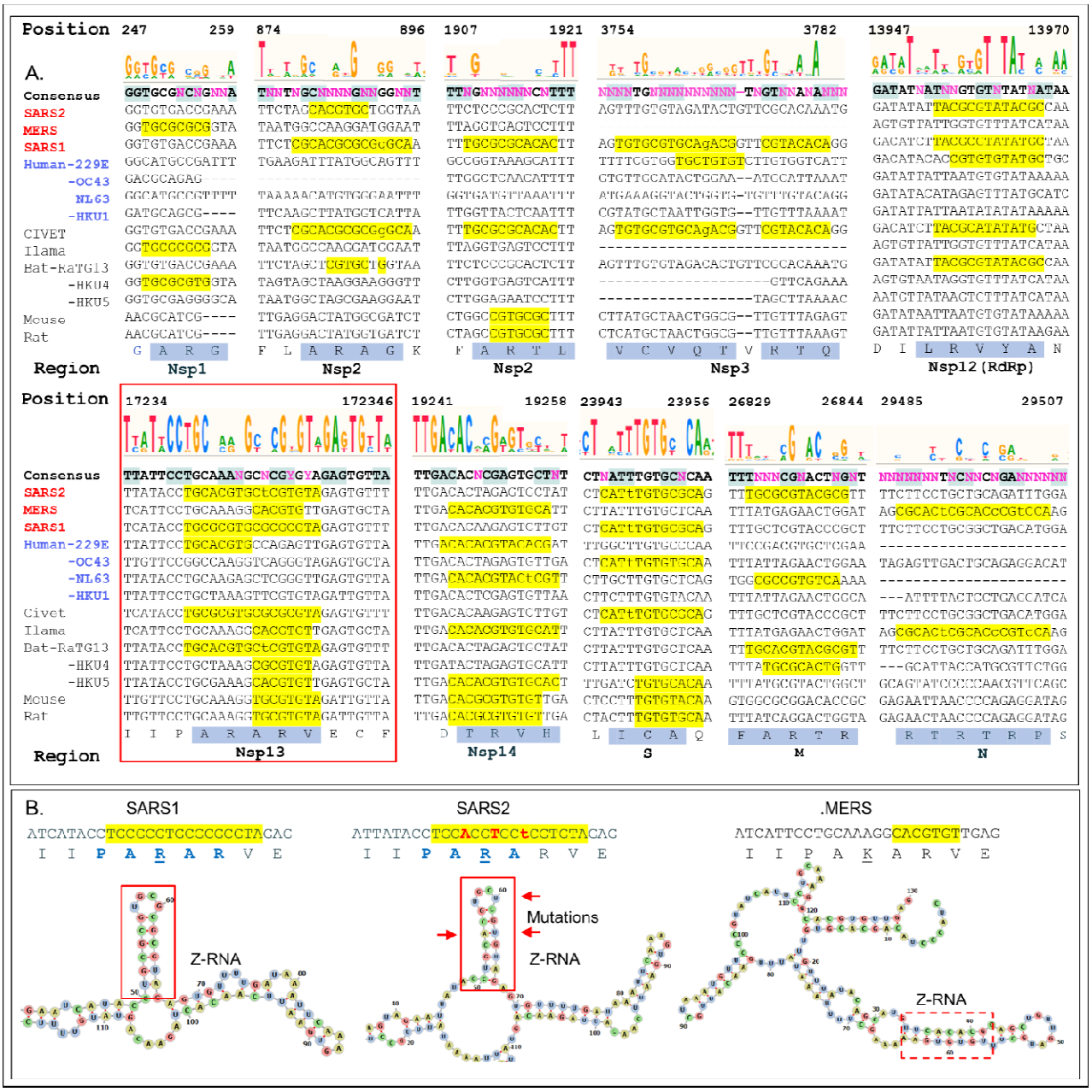

Figure 3 Regions with high ZH3-scores (>600) **A.** The multiple sequence alignment of coronaviruses to SARS2 genome shows potential Z-forming elements in a number of regions of the coronavirus genome. Those encoding Nsp1, Nsp2 and Nsp3 and N proteins contain highly variable regions, while those for the RNA-dependent RNA polymerase (RdRp, Nsp12), the Nsp13 helicase (inside the red box) and the Nsp14 nuclease/methyl-transferase show greater constraint. Lower case letters indicate bases that break the pyrimidine/purine alternation. The amino acid translation of the first and longest nucleotide sequence with a yellow background are highlighted with a blue background. Nucleotide positions are numbered by the SARS2 genome. **B.** Compared to SARS1, the helicase of SAR2 contains three adjacent non-

synonymous mutations that conserve the Z-RNA stem and the peptide sequence, but diminish its Z-forming potential. The equivalent MERS sequence has a very low Z-forming potential and encodes a peptide with a lysine (K) in place of an arginine (R). A potential MERS Z-RNA prone element is close-by (within the dashed box).

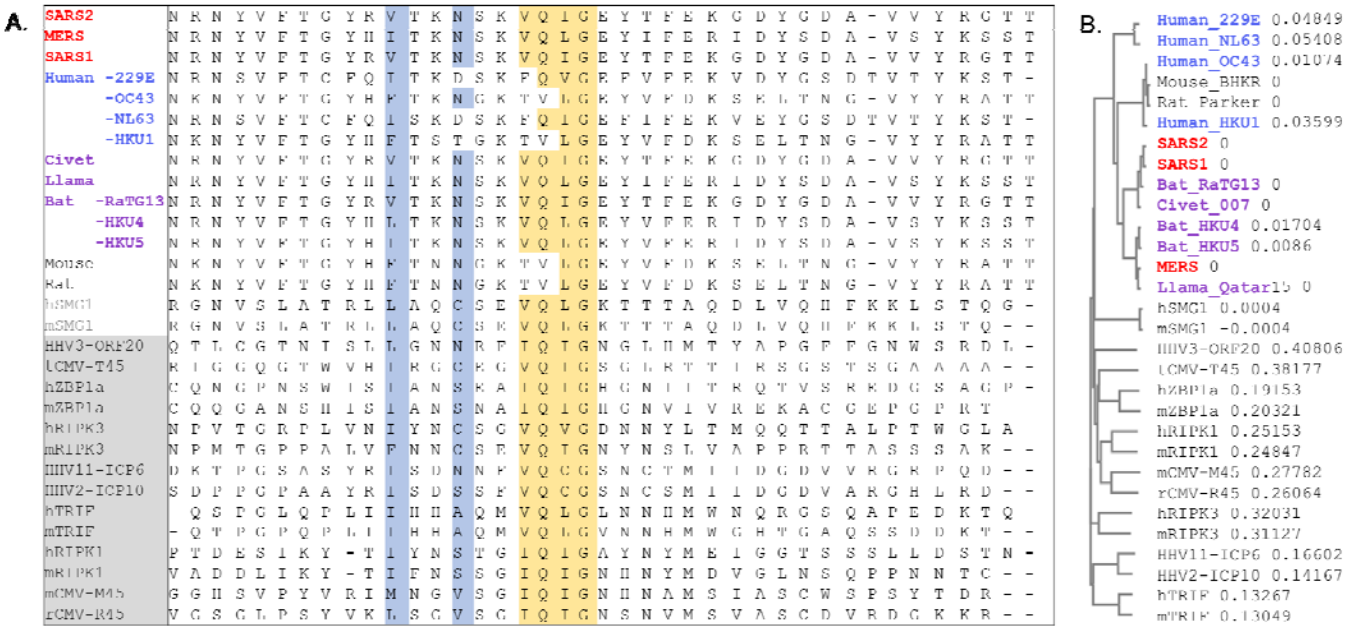

Figure 4. RIP homotypic Interaction motif. **A.** CoV Nsp13 protein sequences from different strains that contain the RHIM (I/V)Q(I/L/V)G residues (in yellow) were aligned with known RHIMs from other viral and host proteins (labels in the gray box). SMG1 was identified here but is not yet a validated RHIM. Residues are colored as in Figure 1. **B.** Cladogram based on distance to show the relationship of proteins. (HHV: human herpes virus; CMV: cytomegalovirus; ZBP1: Z-DNA binding Protein 1; RIPK; Receptor Interacting Protein Kinase; TRIF: Toll like Receptor Adaptor Molecule; SMG: SMG1 nonsense mediated mRNA decay associated PI3K related kinase; h: human; m: mouse; r: rat; t: tupaiid)

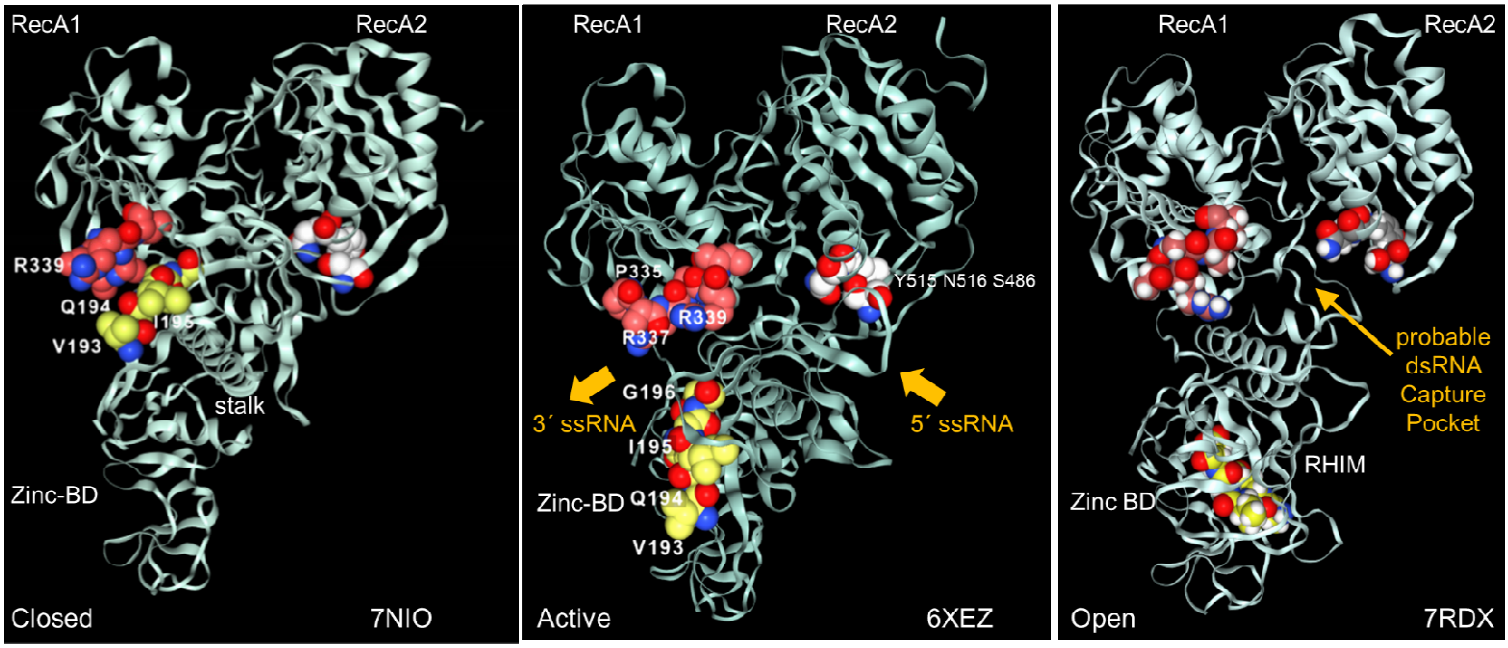

Figure 5 The interaction between the Nsp13 RHIM (residues 193-6) and PARAR (residues 335-9) are conformation dependent. **A.** In the ATP-free apo form of Nsp13, the RHIM (yellow space fill carbons) contacts PARAR (crimson space fill carbons) **B.** In the active state, RHIM and PARAR separate, opening the 5´ end of the single-strand RNA channel, that has the 3´end marked by N516 (white space fill carbons). **C**. In the open complex, the RHIM separates further from the RecA2 domains to create a cavity that is potentially large enough to accommodate dsRNA. This opening is associated with a rotation of the Zinc binding domain (ZincBD) relative to N516. PARAR also rotates, changing the position of R337 and R339. The structures are from PDB files 7NIO [43], 6XEZ [44] and 7RDX [45] as labeled, with images rendered using the NGLViewer [56].

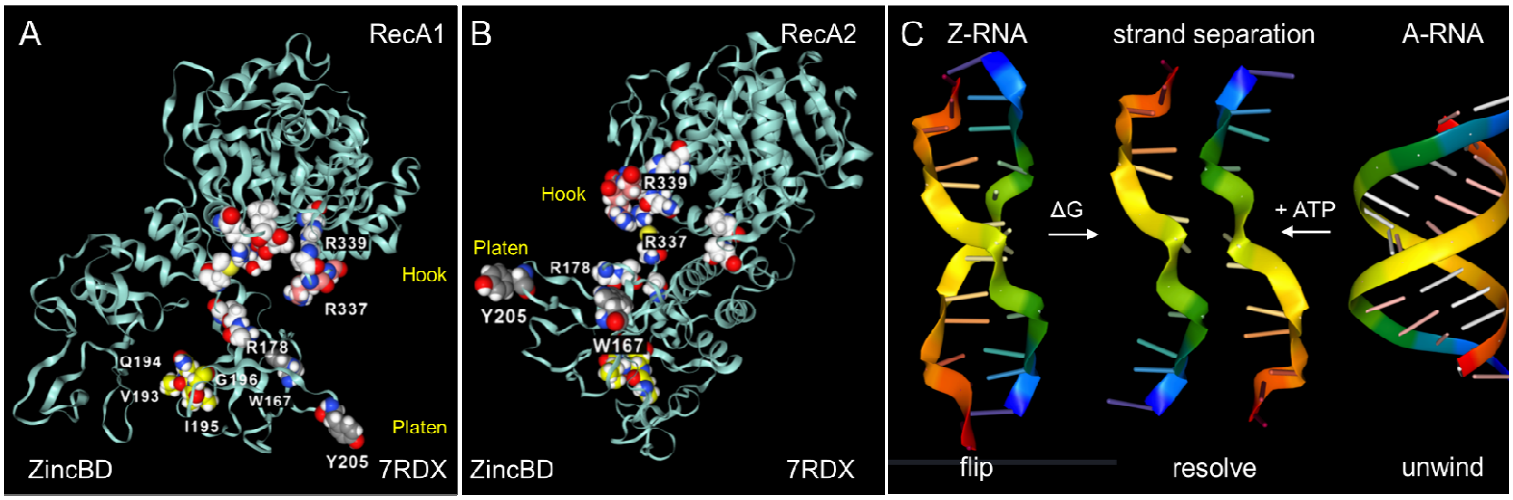

Figure 6 Nsp13 opens to expose a hook and platen for binding dsRNA. **A.** The arginine rich PARAR hook (crimson carbons) and the tyrosine (Y205, grey carbons) platen create a surface for docking dsRNA. Tryptophan (W168)(blue carbons) has the potential to orientate Y205 through and edge to face interaction and create a Z-RNA specific recognition element like that present in the Zα domain and confers specificity for binding to the left-handed helix [61]. In this open orientation, the RHIM (yellow carbons) is free to engage other RHIM proteins. The space fill with white carbons show the residues identified as making base-specific contacts with single-stranded RNA (ssRNA) in the active conformation of Figure 3B (residues 178, 179, 230, 233 in domain 1B, residues 311, 335,361, 362:E,363, 390, 408, 410:E in RecA1). **B.** The view of the Nsp13 molecule from the opposite side to that shown in the first panel. **C.** In addition to the ATP-dependent helicase activity, Nsp13 has the potential to capture ssRNA when Z-RNA flips to and from A-RNA. The higher energy Z-RNA powers the strand-separation, providing the ΔG needed to fuel the Z-flipon helicase activity we refer to as a Z-flipase.

References

[1] L. Galluzzi, I. Vitale, S.A. Aaronson, J.M. Abrams, D. Adam, P. Agostinis, E.S. Alnemri, L. Altucci, I. Amelio, D.W. Andrews, M. Annicchiarico-Petruzzelli, A.V. Antonov, E. Arama, E.H. Baehrecke, N.A. Barlev, N.G. Bazan, F. Bernassola, M.J.M. Bertrand, K. Bianchi, M.V. Blagosklonny, K. Blomgren, C. Borner, P. Boya, C. Brenner, M. Campanella, E. Candi, D. Carmona-Gutierrez, F. Cecconi, F.K. Chan, N.S. Chandel, E.H. Cheng, J.E. Chipuk, J.A. Cidlowski, A. Ciechanover, G.M. Cohen, M. Conrad, J.R. Cubillos-Ruiz, P.E. Czabotar, V. D'Angiolella, T.M. Dawson, V.L. Dawson, V. De Laurenzi, R. De Maria, K.M. Debatin, R.J. DeBerardinis, M. Deshmukh, N. Di Daniele, F. Di Virgilio, V.M. Dixit, S.J. Dixon, C.S. Duckett, B.D. Dynlacht, W.S. El-Deiry, J.W. Elrod, G.M. Fimia, S. Fulda, A.J. Garcia-Saez, A.D. Garg, C. Garrido, E. Gavathiotis, P. Golstein, E. Gottlieb, D.R. Green, L.A. Greene, H. Gronemeyer, A. Gross, G. Hajnoczky, J.M. Hardwick, I.S. Harris, M.O. Hengartner, C. Hetz, H. Ichijo, M. Jaattela, B. Joseph, P.J. Jost, P.P. Juin, W.J. Kaiser, M. Karin, T. Kaufmann, O. Kepp, A. Kimchi, R.N. Kitsis, D.J. Klionsky, R.A. Knight, S. Kumar, S.W. Lee, J.J. Lemasters, B. Levine, A. Linkermann, S.A. Lipton, R.A. Lockshin, C. Lopez-Otin, S.W. Lowe, T. Luedde, E. Lugli, M. MacFarlane, F. Madeo, M. Malewicz, W. Malorni, G. Manic, et al., Molecular

mechanisms of cell death: recommendations of the Nomenclature Committee on Cell Death 2018. Cell Death Differ 25 (2018) 486-541.
[2] A. Herbert, A Genetic Instruction Code Based on DNA Conformation. Trends Genet 35 (2019) 887–890.
[3] A.A. Gulyaeva, and A.E. Gorbalenya, A nidovirus perspective on SARS-CoV-2. Biochem Biophys Res Commun 538 (2021) 24-34.
[4] A.C. Brant, W. Tian, V. Majerciak, W. Yang, and Z.M. Zheng, SARS-CoV-2: from its discovery to genome structure, transcription, and replication. Cell Biosci 11 (2021) 136.
[5] Z. Zhou, Y. Qiu, and X. Ge, The taxonomy, host range and pathogenicity of coronaviruses and other viruses in the Nidovirales order. Anim Dis 1 (2021) 5.
[6] C.E. Comar, S.A. Goldstein, Y. Li, B. Yount, R.S. Baric, and S.R. Weiss, Antagonism of dsRNA-Induced Innate Immune Pathways by NS4a and NS4b Accessory Proteins during MERS Coronavirus Infection. mBio 10 (2019).
[7] G. Mariano, R.J. Farthing, S.L.M. Lale-Farjat, and J.R.C. Bergeron, Structural Characterization of SARS-CoV-2: Where We Are, and Where We Need to Be. Front Mol Biosci 7 (2020) 605236.
[8] Q. Zhang, P. Bastard, Z. Liu, J. Le Pen, M. Moncada-Velez, J. Chen, M. Ogishi, I.K.D. Sabli, S. Hodeib, C. Korol, J. Rosain, K. Bilguvar, J. Ye, A. Bolze, B. Bigio, R. Yang, A.A. Arias, Q. Zhou, Y. Zhang, F. Onodi, S. Korniotis, L. Karpf, Q. Philippot, M. Chbihi, L. Bonnet-Madin, K. Dorgham, N. Smith, W.M. Schneider, B.S. Razooky, H.H. Hoffmann, E. Michailidis, L. Moens, J.E. Han, L. Lorenzo, L. Bizien, P. Meade, A.L. Neehus, A.C. Ugurbil, A. Corneau, G. Kerner, P. Zhang, F. Rapaport, Y. Seeleuthner, J. Manry, C. Masson, Y. Schmitt, A. Schluter, T. Le Voyer, T. Khan, J. Li, J. Fellay, L. Roussel, M. Shahrooei, M.F. Alosaimi, D. Mansouri, H. Al-Saud, F. Al-Mulla, F. Almourfi, S.Z. Al-Muhsen, F. Alsohime, S. Al Turki, R. Hasanato, D. van de Beek, A. Biondi, L.R. Bettini, M. D'Angio, P. Bonfanti, L. Imberti, A. Sottini, S. Paghera, E. Quiros-Roldan, C. Rossi, A.J. Oler, M.F. Tompkins, C. Alba, I. Vandernoot, J.C. Goffard, G. Smits, I. Migeotte, F. Haerynck, P. Soler-Palacin, A. Martin-Nalda, R. Colobran, P.E. Morange, S. Keles, F. Colkesen, T. Ozcelik, K.K. Yasar, S. Senoglu, S.N. Karabela, C. Rodriguez-Gallego, G. Novelli, S. Hraiech, Y. Tandjaoui-Lambiotte, X. Duval, C. Laouenan, C.-S. Clinicians, C. Clinicians, C.G. Imagine, C.C.S.G. French, et al., Inborn errors of type I IFN immunity in patients with life-threatening COVID-19. Science 370 (2020).
[9] P. Bastard, L.B. Rosen, Q. Zhang, E. Michailidis, H.H. Hoffmann, Y. Zhang, K. Dorgham, Q. Philippot, J. Rosain, V. Beziat, J. Manry, E. Shaw, L. Haljasmagi, P. Peterson, L. Lorenzo, L. Bizien, S. Trouillet-Assant, K. Dobbs, A.A. de Jesus, A. Belot, A. Kallaste, E. Catherinot, Y. Tandjaoui-Lambiotte, J. Le Pen, G. Kerner, B. Bigio, Y. Seeleuthner, R. Yang, A. Bolze, A.N. Spaan, O.M. Delmonte, M.S. Abers, A. Aiuti, G. Casari, V. Lampasona, L. Piemonti, F. Ciceri, K. Bilguvar, R.P. Lifton, M. Vasse, D.M. Smadja, M. Migaud, J. Hadjadj, B. Terrier, D. Duffy, L. Quintana-Murci, D. van de Beek, L. Roussel, D.C. Vinh, S.G. Tangye, F. Haerynck, D. Dalmau, J. Martinez-Picado, P. Brodin, M.C. Nussenzweig, S. Boisson-Dupuis, C. Rodriguez-Gallego, G. Vogt, T.H. Mogensen, A.J. Oler, J. Gu, P.D. Burbelo, J.I. Cohen, A. Biondi, L.R. Bettini, M. D'Angio, P. Bonfanti, P. Rossignol, J. Mayaux, F. Rieux-Laucat, E.S. Husebye, F. Fusco, M.V. Ursini, L. Imberti, A. Sottini, S. Paghera, E. Quiros-Roldan, C. Rossi, R. Castagnoli, D. Montagna, A. Licari, G.L. Marseglia, X. Duval, J. Ghosn, H. Lab, N.-U.I.R.t.C. Group, C. Clinicians, C.-S. Clinicians, C.G. Imagine, C.C.S.G. French, C. Milieu Interieur, V.C.C. Co, U.M.C.C.-B. Amsterdam, C.H.G. Effort, J.S. Tsang, R. Goldbach-Mansky, K. Kisand, M.S. Lionakis, A. Puel, S.Y. Zhang, et al., Autoantibodies against type I IFNs in patients with life-threatening COVID-19. Science 370 (2020).
[10] X. Solanich, R. Rigo-Bonnin, V.D. Gumucio, P. Bastard, J. Rosain, Q. Philippot, X.L. Perez-Fernandez, M.P. Fuset-Cabanes, M.A. Gordillo-Benitez, G. Suarez-Cuartin, E. Boza-Hernandez, A. Riera-Mestre, A. Parra-Martinez, R. Colobran, A. Antoli, S. Navarro, G. Rocamora-Blanch, M. Framil, L. Calatayud, X. Corbella, J.L. Casanova, F. Morandeira, and J. Sabater-Riera, Pre-existing

Autoantibodies Neutralizing High Concentrations of Type I Interferons in Almost 10% of COVID-19 Patients Admitted to Intensive Care in Barcelona. J Clin Immunol 41 (2021) 1733-1744.
[11] G. Wolff, C.E. Melia, E.J. Snijder, and M. Barcena, Double-Membrane Vesicles as Platforms for Viral Replication. Trends Microbiol 28 (2020) 1022-1033.
[12] S. Hussain, J. Pan, Y. Chen, Y. Yang, J. Xu, Y. Peng, Y. Wu, Z. Li, Y. Zhu, P. Tien, and D. Guo, Identification of novel subgenomic RNAs and noncanonical transcription initiation signals of severe acute respiratory syndrome coronavirus. J Virol 79 (2005) 5288-95.
[13] A. Herbert, Z-DNA and Z-RNA in human disease. Communications Biology 2 (2019) 7.
[14] A. Herbert, To "Z" or not to "Z": Z-RNA, self-recognition, and the MDA5 helicase. PLoS Genet 17 (2021) e1009513.
[15] P.S. Ho, Thermogenomics: thermodynamic-based approaches to genomic analyses of DNA structure. Methods 47 (2009) 159-67.
[16] P.J. Nichols, S. Bevers, M. Henen, J.S. Kieft, Q. Vicens, and B. Vögeli, Recognition of non-CpG repeats in Alu and ribosomal RNAs by the Z-RNA binding domain of ADAR1 induces A-Z junctions. Nat Commun 12 (2021).
[17] A. Herbert, J. Alfken, Y.G. Kim, I.S. Mian, K. Nishikura, and A. Rich, A Z-DNA binding domain present in the human editing enzyme, double-stranded RNA adenosine deaminase. Proc Natl Acad Sci U S A 94 (1997) 8421-6.
[18] A. Athanasiadis, Zα-domains: At the intersection between RNA editing and innate immunity. Seminars in Cell & Developmental Biology 23 (2012) 275-280.
[19] L. Sun, Y. Miao, Z. Wang, H. Chen, P. Dong, H. Zhang, L. Wu, M. Jiang, L. Chen, W. Yang, P. Lin, D. Jing, Z. Luo, Y. Zhang, Y.S. Jung, X. Wu, Y. Qian, and Y. Wu, Structural insight into African Swine Fever Virus I73R protein reveals it as a Z-DNA binding protein. Transbound Emerg Dis (2022).
[20] H. Guo, S. Omoto, P.A. Harris, J.N. Finger, J. Bertin, P.J. Gough, W.J. Kaiser, and E.S. Mocarski, Herpes simplex virus suppresses necroptosis in human cells. Cell Host Microbe 17 (2015) 243-51.
[21] Z. Huang, S.Q. Wu, Y. Liang, X. Zhou, W. Chen, L. Li, J. Wu, Q. Zhuang, C. Chen, J. Li, C.Q. Zhong, W. Xia, R. Zhou, C. Zheng, and J. Han, RIP1/RIP3 binding to HSV-1 ICP6 initiates necroptosis to restrict virus propagation in mice. Cell Host Microbe 17 (2015) 229-42.
[22] X. Sun, J. Yin, M.A. Starovasnik, W.J. Fairbrother, and V.M. Dixit, Identification of a novel homotypic interaction motif required for the phosphorylation of receptor-interacting protein (RIP) by RIP3. J Biol Chem 277 (2002) 9505-11.
[23] F.K. Chan, N.F. Luz, and K. Moriwaki, Programmed necrosis in the cross talk of cell death and inflammation. Annu Rev Immunol 33 (2015) 79-106.
[24] M. Mompean, W. Li, J. Li, S. Laage, A.B. Siemer, G. Bozkurt, H. Wu, and A.E. McDermott, The Structure of the Necrosome RIPK1-RIPK3 Core, a Human Hetero-Amyloid Signaling Complex. Cell 173 (2018) 1244-1253 e10.
[25] C.L. Pham, N. Shanmugam, M. Strange, A. O'Carroll, J.W. Brown, E. Sierecki, Y. Gambin, M. Steain, and M. Sunde, Viral M45 and necroptosis-associated proteins form heteromeric amyloid assemblies. EMBO Rep 20 (2019).
[26] X. Wu, Y. Ma, K. Zhao, J. Zhang, Y. Sun, Y. Li, X. Dong, H. Hu, J. Liu, J. Wang, X. Zhang, B. Li, H. Wang, D. Li, B. Sun, J. Lu, and C. Liu, The structure of a minimum amyloid fibril core formed by necroptosis-mediating RHIM of human RIPK3. Proc Natl Acad Sci U S A 118 (2021).
[27] T. Zhang, C. Yin, D.F. Boyd, G. Quarato, J.P. Ingram, M. Shubina, K.B. Ragan, T. Ishizuka, J.C. Crawford, B. Tummers, D.A. Rodriguez, J. Xue, S. Peri, W.J. Kaiser, C.B. Lopez, Y. Xu, J.W. Upton, P.G. Thomas, D.R. Green, and S. Balachandran, Influenza Virus Z-RNAs Induce ZBP1-Mediated Necroptosis. Cell 180 (2020) 1115-1129.

[28] H. Koehler, S. Cotsmire, T. Zhang, S. Balachandran, J.W. Upton, J. Langland, D. Kalman, B.L. Jacobs, and E.S. Mocarski, Vaccinia virus E3 prevents sensing of Z-RNA to block ZBP1-dependent necroptosis. Cell Host Microbe (2021).
[29] E.S. Mocarski, W.J. Kaiser, D. Livingston-Rosanoff, J.W. Upton, and L.P. Daley-Bauer, True grit: programmed necrosis in antiviral host defense, inflammation, and immunogenicity. J Immunol 192 (2014) 2019-26.
[30] G.P. Schroth, P.J. Chou, and P.S. Ho, Mapping Z-DNA in the human genome. Computer-aided mapping reveals a nonrandom distribution of potential Z-DNA-forming sequences in human genes. J Biol Chem 267 (1992) 11846-55.
[31] T.S. Bayer, L.N. Booth, S.M. Knudsen, and A.D. Ellington, Arginine-rich motifs present multiple interfaces for specific binding by RNA. Rna 11 (2005) 1848-57.
[32] H. Slanina, R. Madhugiri, G. Bylapudi, K. Schultheiss, N. Karl, A. Gulyaeva, A.E. Gorbalenya, U. Linne, and J. Ziebuhr, Coronavirus replication-transcription complex: Vital and selective NMPylation of a conserved site in nsp9 by the NiRAN-RdRp subunit. Proc Natl Acad Sci U S A 118 (2021).
[33] N.S. Ogando, J.C. Zevenhoven-Dobbe, Y. van der Meer, P.J. Bredenbeek, C.C. Posthuma, E.J. Snijder, and T. Gallagher, The Enzymatic Activity of the nsp14 Exoribonuclease Is Critical for Replication of MERS-CoV and SARS-CoV-2. J Virol 94 (2020).
[34] I.G. Madu, S. Belouzard, and G.R. Whittaker, SARS-coronavirus spike S2 domain flanked by cysteine residues C822 and C833 is important for activation of membrane fusion. Virology 393 (2009) 265-71.
[35] D. Schoeman, and B.C. Fielding, Coronavirus envelope protein: current knowledge. Virol J 16 (2019) 69.
[36] A.S. Mendez, M. Ly, A.M. Gonzalez-Sanchez, E. Hartenian, N.T. Ingolia, J.H. Cate, and B.A. Glaunsinger, The N-terminal domain of SARS-CoV-2 nsp1 plays key roles in suppression of cellular gene expression and preservation of viral gene expression. Cell Rep 37 (2021) 109841.
[37] M. Gupta, C.M. Azumaya, M. Moritz, S. Pourmal, A. Diallo, G.E. Merz, G. Jang, M. Bouhaddou, A. Fossati, A.F. Brilot, D. Diwanji, E. Hernandez, N. Herrera, H.T. Kratochvil, V.L. Lam, F. Li, Y. Li, H.C. Nguyen, C. Nowotny, T.W. Owens, J.K. Peters, A.N. Rizo, U. Schulze-Gahmen, A.M. Smith, I.D. Young, Z. Yu, D. Asarnow, C. Billesbolle, M.G. Campbell, J. Chen, K.H. Chen, U.S. Chio, M.S. Dickinson, L. Doan, M. Jin, K. Kim, J. Li, Y.L. Li, E. Linossi, Y. Liu, M. Lo, J. Lopez, K.E. Lopez, A. Mancino, F.R. Moss, M.D. Paul, K.I. Pawar, A. Pelin, T.H. Pospiech, C. Puchades, S.G. Remesh, M. Safari, K. Schaefer, M. Sun, M.C. Tabios, A.C. Thwin, E.W. Titus, R. Trenker, E. Tse, T.K.M. Tsui, F. Wang, K. Zhang, Y. Zhang, J. Zhao, F. Zhou, Y. Zhou, L. Zuliani-Alvarez, Q.S.B. Consortium, D.A. Agard, Y. Cheng, J.S. Fraser, N. Jura, T. Kortemme, A. Manglik, D.R. Southworth, R.M. Stroud, D.L. Swaney, N.J. Krogan, A. Frost, O.S. Rosenberg, and K.A. Verba, CryoEM and AI reveal a structure of SARS-CoV-2 Nsp2, a multifunctional protein involved in key host processes. bioRxiv (2021).
[38] J. Lei, Y. Kusov, and R. Hilgenfeld, Nsp3 of coronaviruses: Structures and functions of a large multi-domain protein. Antiviral Res 149 (2018) 58-74.
[39] T.H.V. Nguyen, J. Lichiere, B. Canard, N. Papageorgiou, S. Attoumani, F. Ferron, and B. Coutard, Structure and oligomerization state of the C-terminal region of the Middle East respiratory syndrome coronavirus nucleoprotein. Acta Crystallogr D Struct Biol 75 (2019) 8-15.
[40] H. Takeuchi, N. Hanamura, H. Hayasaka, and I. Harada, B-Z transition of poly(dG-m5dC) induced by binding of Lys-containing peptides. FEBS Lett 279 (1991) 253-5.
[41] K.T. Powers, J.A. Szeto, and C. Schaffitzel, New insights into no-go, non-stop and nonsense-mediated mRNA decay complexes. Curr Opin Struct Biol 65 (2020) 110-118.
[42] J.-L.E.P.H. Darlix, A.O. Adedeji, B. Marchand, A.J.W. te Velthuis, E.J. Snijder, S. Weiss, R.L. Eoff, K. Singh, and S.G. Sarafianos, Mechanism of Nucleic Acid Unwinding by SARS-CoV Helicase. PLoS One 7 (2012).

[43] J.A. Newman, A. Douangamath, S. Yadzani, Y. Yosaatmadja, A. Aimon, J. Brandao-Neto, L. Dunnett, T. Gorrie-Stone, R. Skyner, D. Fearon, M. Schapira, F. von Delft, and O. Gileadi, Structure, mechanism and crystallographic fragment screening of the SARS-CoV-2 NSP13 helicase. Nat Commun 12 (2021) 4848.
[44] J. Chen, B. Malone, E. Llewellyn, M. Grasso, P.M.M. Shelton, P.D.B. Olinares, K. Maruthi, E.T. Eng, H. Vatandaslar, B.T. Chait, T.M. Kapoor, S.A. Darst, and E.A. Campbell, Structural Basis for Helicase-Polymerase Coupling in the SARS-CoV-2 Replication-Transcription Complex. Cell 182 (2020) 1560-1573 e13.
[45] J. Chen, Q. Wang, B. Malone, E. Llewellyn, Y. Pechersky, K. Maruthi, E.T. Eng, J.K. Perry, E.A. Campbell, D.E. Shaw, and S.A. Darst, Ensemble cryo-electron microscopy reveals conformational states of the nsp13 helicase in the SARS-CoV-2 helicase replication-transcription complex. bioRxiv (2021) 2021.11.10.468168.
[46] S.N. Palmer, S. Chappidi, C. Pinkham, D.C. Hancks, and T. Leitner, Evolutionary Profile for (Host and Viral) MLKL Indicates Its Activities as a Battlefront for Extensive Counteradaptation. Mol Biol Evol 38 (2021) 5405-5422.
[47] A. Herbert, A. Fedorov, and M. Poptsova, Mono a Mano: ZBP1's Love-Hate Relationship with the Kissing Virus. Int J Mol Sci 23 (2022).
[48] N. Shanmugam, M. Baker, M. Sanz-Hernandez, E. Sierecki, Y. Gambin, M. Steain, C.L.L. Pham, and M. Sunde, Herpes simplex virus encoded ICP6 protein forms functional amyloid assemblies with necroptosis-associated host proteins. Biophys Chem 269 (2021) 106524.
[49] M. Mompean, G. Bozkurt, and H. Wu, Mimicry by a viral RHIM. EMBO Rep 20 (2019).
[50] M. Steain, M. Baker, C.L.L. Pham, N. Shanmugam, Y. Gambin, E. Sierecki, B.P. McSharry, S. Avdic, B. Slobedman, M. Sunde, and A. Abendroth, Varicella zoster virus encodes a viral decoy RHIM to inhibit cell death. PLoS Pathog 16 (2020) e1008473.
[51] M.O. Ullah, M.J. Sweet, A. Mansell, S. Kellie, and B. Kobe, TRIF-dependent TLR signaling, its functions in host defense and inflammation, and its potential as a therapeutic target. Journal of Leukocyte Biology 100 (2016) 27-45.
[52] A.L. Totura, A. Whitmore, S. Agnihothram, A. Schafer, M.G. Katze, M.T. Heise, and R.S. Baric, Toll-Like Receptor 3 Signaling via TRIF Contributes to a Protective Innate Immune Response to Severe Acute Respiratory Syndrome Coronavirus Infection. mBio 6 (2015) e00638-15.
[53] M.W. Popp, H. Cho, and L.E. Maquat, Viral subversion of nonsense-mediated mRNA decay. Rna 26 (2020) 1509-1518.
[54] M. Buhler, S. Steiner, F. Mohn, A. Paillusson, and O. Muhlemann, EJC-independent degradation of nonsense immunoglobulin-mu mRNA depends on 3' UTR length. Nat Struct Mol Biol 13 (2006) 462-4.
[55] S. Li, Y. Zhang, Z. Guan, H. Li, M. Ye, X. Chen, J. Shen, Y. Zhou, Z.L. Shi, P. Zhou, and K. Peng, SARS-CoV-2 triggers inflammatory responses and cell death through caspase-8 activation. Signal Transduct Target Ther 5 (2020) 235.
[56] A.S. Rose, and P.W. Hildebrand, NGL Viewer: a web application for molecular visualization. Nucleic Acids Res 43 (2015) W576-9.
[57] R.C. Edgar, MUSCLE: multiple sequence alignment with high accuracy and high throughput. Nucleic Acids Res 32 (2004) 1792-7.
[58] T.L. Bailey, J. Johnson, C.E. Grant, and W.S. Noble, The MEME Suite. Nucleic Acids Res 43 (2015) W39-W49.
[59] K. Katoh, and D.M. Standley, MAFFT multiple sequence alignment software version 7: improvements in performance and usability. Mol Biol Evol 30 (2013) 772-80.
[60] R. Lorenz, S.H. Bernhart, C. Honer Zu Siederdissen, H. Tafer, C. Flamm, P.F. Stadler, and I.L. Hofacker, ViennaRNA Package 2.0. Algorithms Mol Biol 6 (2011) 26.

[61] T. Schwartz, M.A. Rould, K. Lowenhaupt, A. Herbert, and A. Rich, Crystal structure of the Zα domain of the human editing enzyme ADAR1 bound to left-handed Z-DNA. Science 284 (1999) 1841-5.